Utilizing Heat of Wetting to Estimate Physical Properties of Tuff

Kristopher Kuhlman[1], Forest T Good[2], Melissa M Mills[1], Matthew J Paul[1], Jason E Heath[3], Tara Laforce[4], and Brittney D Seaburn[1]

[1]Sandia National Laboratories Nuclear Waste Disposal Research & Analysis
[2]New Mexico Tech
[3]Sandia National Laboratories Geomechanics
[4]Sandia National Laboratories Applied Systems Analysis & Research

January 15, 2024

Abstract

During characterization efforts of complex sites and geologies, it is important to estimate material properties efficiently and robustly. We present data and modeling related to the heat of wetting process during spontaneous imbibition, as observed in zeolitic tuff. The heat of wetting is due to adsorption of liquid water and water vapor to an oven-dry core sample and results in an observable temperature rise. The fitting of numerical models to imbibition observations allows simultaneous constraint of single-phase (porosity, permeability), two-phase (van Genuchten m and alpha), thermal (thermal diffusivity), and transport (tortuosity) properties from a single imbibition test. Petrographic analysis informs how microstructure connectivity and pore-lining phases affect the imbibition process. Estimating multiple properties simultaneously from a single test on a core sample helps ensure consistency in interpreted material properties. SNL is managed and operated by NTESS under DOE NNSA contract DE-NA0003525 (SAND2023-07021A).

Sandia National Laboratories

Utilizing Heat of Wetting to Estimate Physical Properties of Tuff

American Geophysical Union 2023 Fall Meeting
H11S-1501

Kristopher L. Kuhlman[1], Forest T. Good[1,4], Melissa M. Mills[1], Matthew J. Paul[1], Jason E. Heath[2], Tara LaForce[3], Brittney D. Seaburn[1]
Sandia National Laboratories: [1]Nuclear Waste Disposal Research & Analysis, [2]Geomechanics, [3]Applied Systems Analysis & Research; [4]New Mexico Institute of Mining and Technology

1. Background and Zeolitic Test Results

We need to estimate two-phase flow properties for vadose zone rocks for site characterization efforts, especially for gas transport in the vadose zone from an underground explosion (Heath et al., 2021). Kuhlman et al. (2022b) adapted an approach proposed by Peters et al. (1987) to estimate properties from transient imbibition experiments. It traded a more complex test interpretation (i.e., numerical model and parameter estimation) for simpler test execution in the laboratory (i.e., a single transient imbibition test). To constrain the model, the test monitors uptake of water by a sample while tracking the progress of the wetting front height.

Previous work (Kuhlman et al., 2022b) monitored the wetting front progress with images. We monitored the change in temperature in the core using resistance temperature detectors (RTDs) attached to the sample with rubber bands (**Fig 1**).

The imbibition test measured the mass loss from a constant-head Mariotte bottle (**Fig 2**), while monitoring the temperature at locations along the sides of the sample. Electrical resistance across the sample itself was also measured.

For zeolitic tuff cores (up to 60% zeolite minerals like clinoptilolite), there was a clear separation observed between the arrival of the visible wetting front and the arrival of the thermal front. The wetting front height was estimated from images and from the mass of water imbibed data (**Fig 3**).

Fig 1. Zeolitic tuff core sample (left) with RTDs attached (right) used in imbibition experiments.

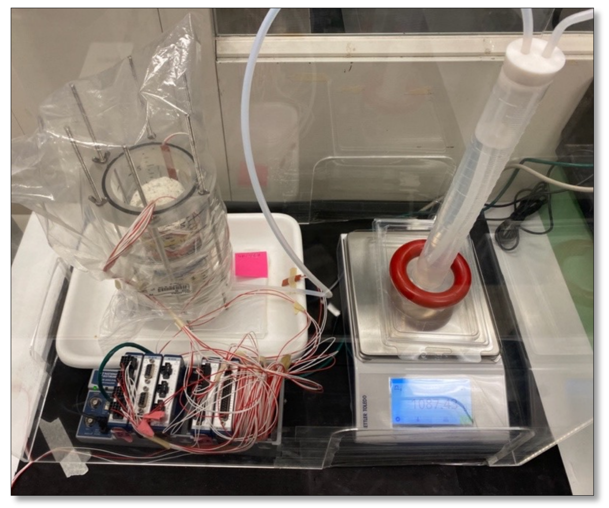

Fig 2. Sandia thermal imbibition test setup. Sample holder (upper left), Mariotte bottle on balance (right), and data acquisition (lower left); Kuhlman et al. (2022)

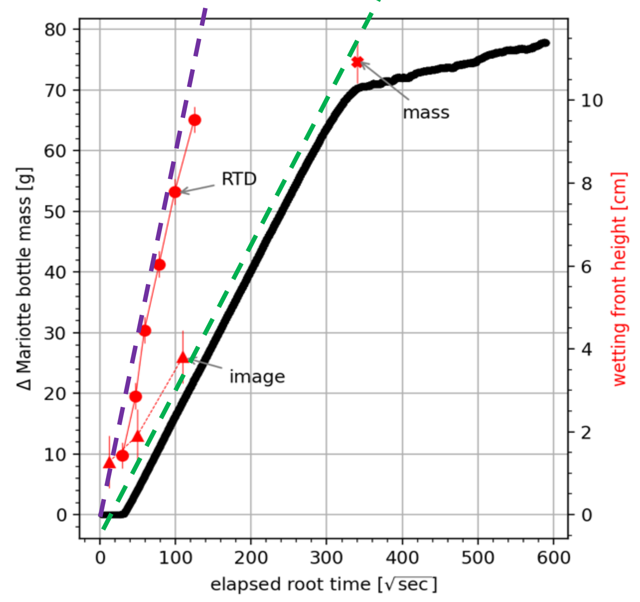

Fig 3. Mass imbibed (black) wetting front observed visually (▲) and via RTDs (●) vs. root time for zeolitic tuff core. Green line is $7.46{\times}10^{-5}$ m/$\sqrt{s}$ slope

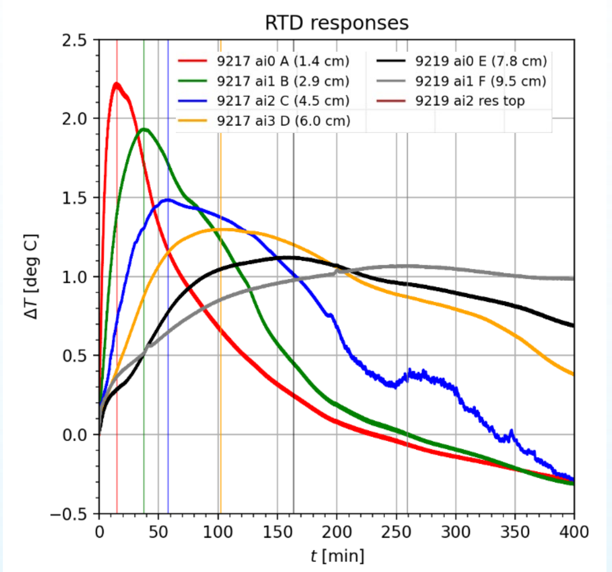

Fig 4. Temperature change in zeolitic core (Good et al., 2023)

The data from zeolitic core indicated two clear speeds of fronts moving up the sample (slopes of dashed lines in **Fig 3**). Faster transport was associated with first arrival of a temperature peak (purple line, 4.3 hours to top RTD), while slower transport was associated with the arrival of liquid water at a point in the sample (green line, 25 hours to top RTD).

The time to peak temperature at each location (**Fig 4**) are each plotted with position on **Fig 3** as red circles (Kuhlman et al., 2022a).

2. Physical Processes

Spontaneous imbibition of water into porous media is an exothermic process. This can be caused by two processes: adsorption of water vapor or adhesion of liquid water (i.e., immersion). These are like phase-change processes (**Fig 5**).

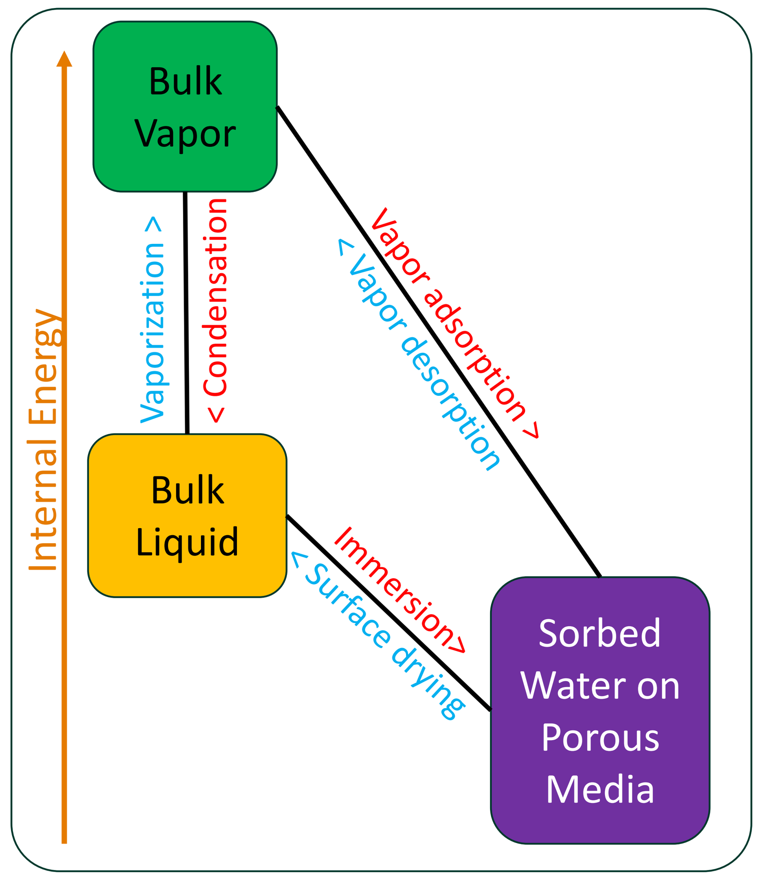

Fig 5. Phase changes in a microporous medium. Exothermic processes are red, endothermic processes are blue.

Zeolites are common alteration products where weathering of volcanic glass occurs. Zeolites have cage-like molecular structures which can trap some molecules.

Gas molecules that adsorb onto a wetting surface are at a lower chemical potential than the bulk state, releasing thermal energy. The cage-like structure of zeolites may present an even lower chemical potential than planar surfaces, resulting in a comparatively large release of energy for vapor adsorption (Żołądek-Nowak et al., 2012).

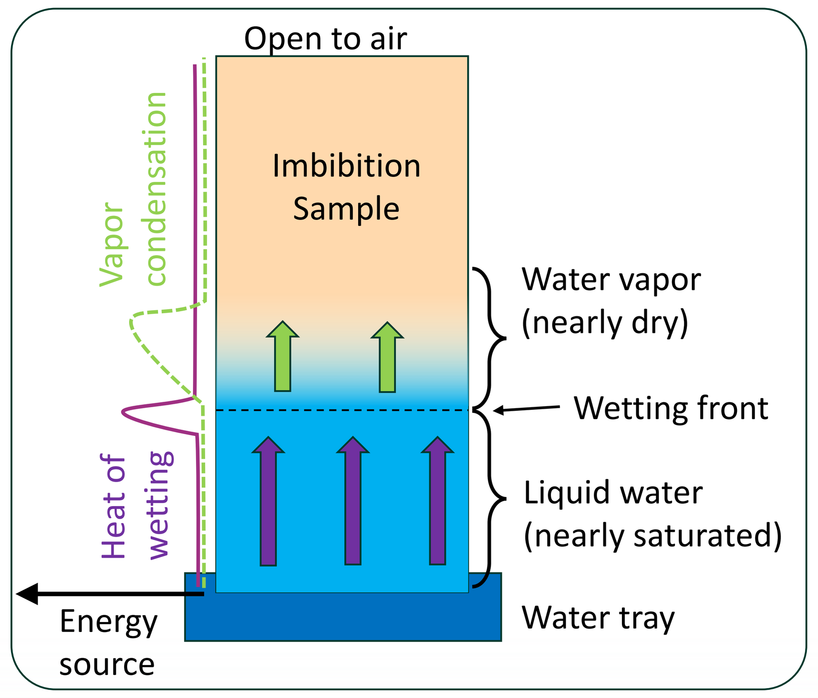

Fig 6 illustrates the two mechanisms that release energy during an imbibition test.

Heat of wetting releases sensible heat at the wetting front (Murali et al., 2020), while vapor condensation releases sensible heat in the visible dry part of the sample ahead of the wetting front.

Fig 6. Diagram (left) showing relative locations where heat of wetting and vapor condensation occur.

Fig 7 shows the process in a high-permeability core (Boise sandstone); with infrared images to visualize temperature distribution across the core during the imbibition process.

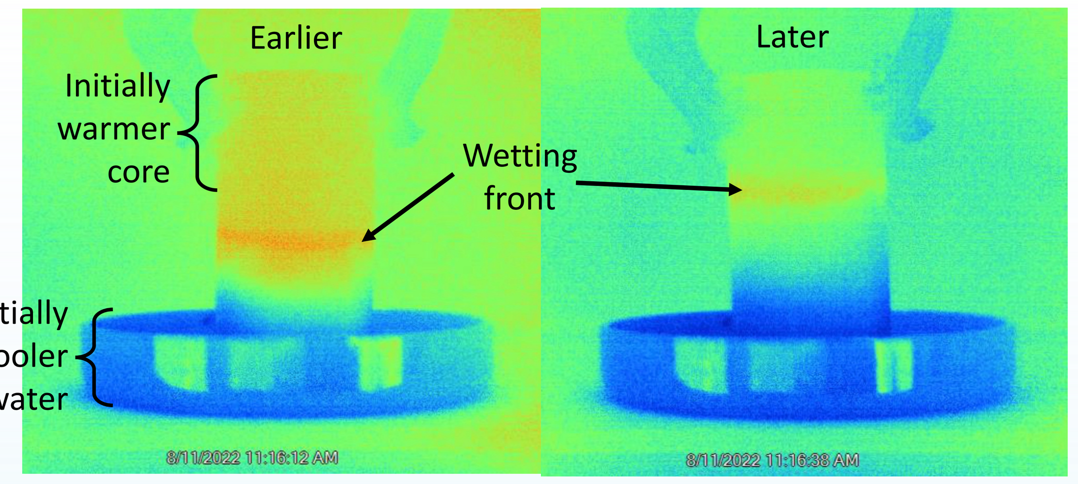

Fig 7. Infrared images during imbibition into Boise sandstone core (3 cm diameter). Warmest place at both times is at wetting front.

Cooler water imbibes into a room-temperature core. The water is slightly cooler due to evaporative effects. The infrared images clearly show the warmest place is the leading edge of the wetting front (warmer than the core or the water were initially). In this sample vapor migration ahead of the wetting front is minimal.

3. Vitric Tuff Results

For contrast against tests conducted in zeolitic tuff samples (**Fig 1** & **Fig 3**), a vitric tuff sample was also tested. The wetting front took approximately 1 hour to imbibe to the top of the 17.5 cm long vitric tuff sample.

Fig 8 shows RTD and electrical resistance measurements acquired using a NI cDAQ. The RTD's were measured using 9219 and 9217 NI cModules), while electrical resistance measurements were measured using a Keithley 2604b source meter through a WireFlow 3132 multiplexer. The measured electrical resistance drops two orders of magnitude when the wetting front moves past an observation point. Photos were also used to estimate the wetting front elevation (**Fig 9**).

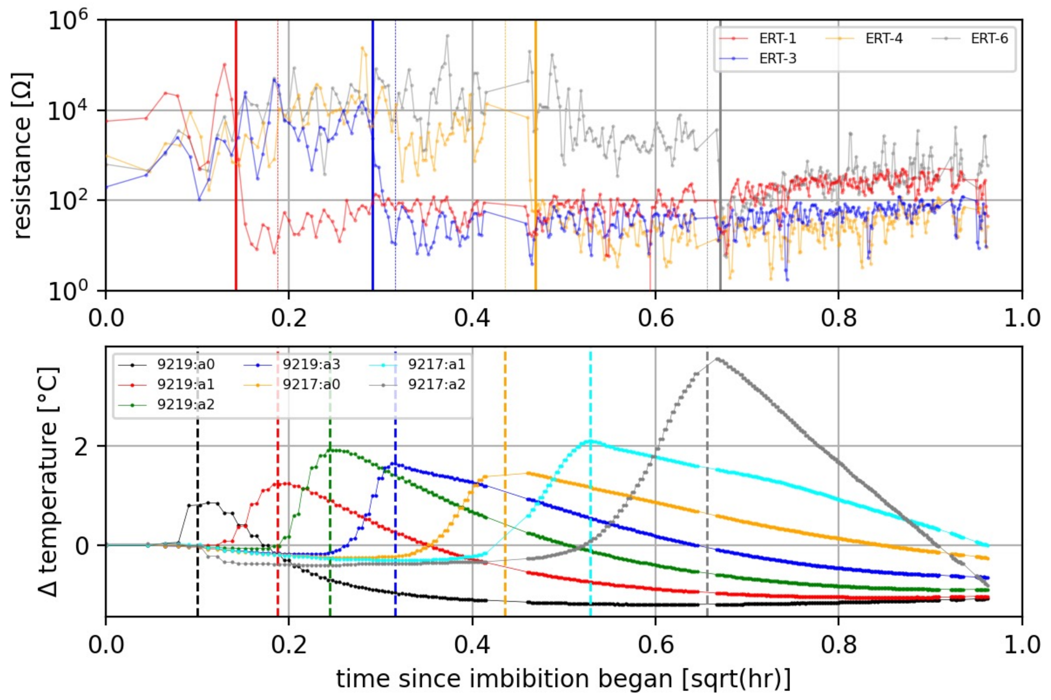

Fig 8. Temperature rise using RTDs (bottom) and resistance (top) vs. square root time for vitric tuff core

Vertical lines in **Fig 8** at the resistance drop (top) and peak temperature (bottom), along with times and heights are plotted as points in **Fig 10**. The three types of data clearly are similar for this vitric core, where vapor migration ahead of the wetting front it minimal.

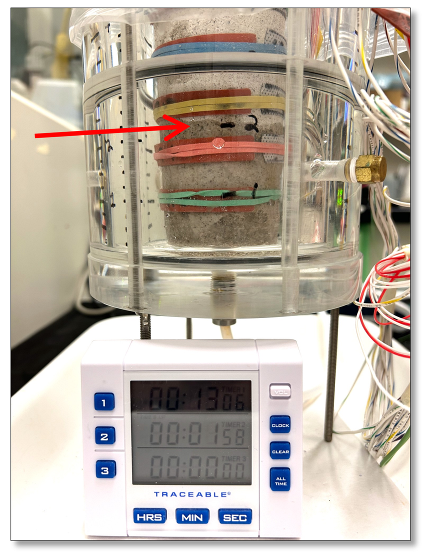

Fig 9. Photo of wetting front (red arrow) in vitric tuff core with RTD and resistance measurements.

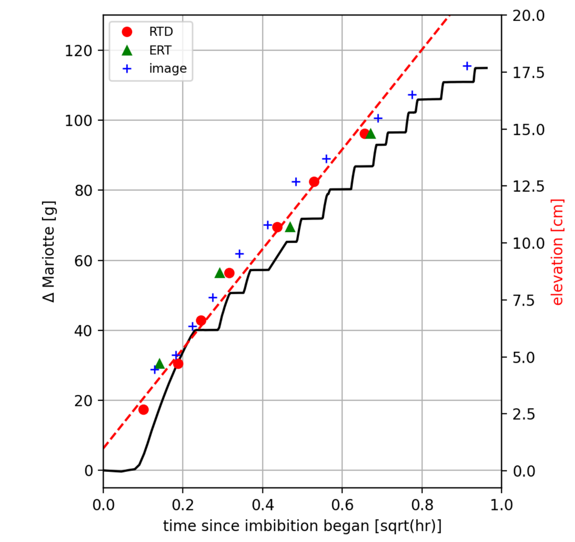

Fig 10. RTD (●), resistance (▲), and image (+) data showing wetting front progress. Line is $3.65{\times}10^{-3}$ m/$\sqrt{s}$ slope

The slope of the line in **Fig 10** is the sorptivity, S, (Philip, 1957), which has been related to the intrinsic permeability via regression methods (Tokunaga, 2020; equation to right). Here $\eta = 8.9{\times}10^{-4}$ [Pa · s] is viscosity, $\Delta\theta$ is the change in liquid saturation, and $j_2 = 0.0912$ [Pa · m$^{0.72}$].

$$k = \left(\frac{\eta}{2 j_2 \triangle \theta}\right)^{1.56} S^{3.12}$$

The change in water-filled porosity (0.245) is estimated from the mass of water imbibed (120 g) and the sample volume (490 cm^3).

The vitric tuff (**Fig 10**) has an estimated permeability of $3.1{\times}10^{-14}$ m^2, while the zeolitic tuff in (**Fig 3**) has an estimated permeability of $3.4{\times}10^{-16}$ m^2. These two samples illustrate the method applied to both high permeability (vitric) and low permeability (zeolitic) tuff samples.

4. Future Directions

Using RTDs and electrodes, data can be fit to an analytical solution (Good et al., 2023) or numerical models (Kuhlman et al., 2022b). This approach could be used to estimate flow (porosity, permeability), transport (tortuosity), and thermal (diffusivity) properties from one lab test.

References

Good, F. T., Kuhlman, K. L., LaForce, T. C., Paul, M. J., & Heath, J. E. (2023). Analytical solution and parameter estimation for heat of wetting and vapor adsorption during spontaneous imbibition in tuff. *International Journal of Heat and Mass Transfer*, 203, 123814.

Heath, J.E. & K.L. Kuhlman, S.T. Broome, J.E. Wilson & B. Malama, 2021. Heterogeneous multiphase flow properties of volcanic rocks and implications for noble gas transport from underground nuclear explosions, *Vadose Zone Journal, 20*(3):e20123.

Kuhlman, K.L., M.M. Mills, J.E. Heath & M.J. Paul, 2022a. *FY22 Progress on Multicontinuum Methods in Containment. Sandia National Laboratories*. doi:10.2172/1877460.

Kuhlman, K.L., M.M. Mills, J.E. Heath, M.J. Paul, J.E. Wilson & J.E. Bower, 2022b. Parameter estimation from spontaneous imbibition into volcanic tuff, *Vadose Zone Journal, 21*(2):e20188.

Murali, V., Zeegers, J. C., & Darhuber, A. A. (2020). Infrared thermography of sorptive heating of thin porous media–Experiments and continuum simulations. *International Journal of Heat and Mass Transfer*, 147, 118875.

Peters, R.R., E.A. Klavetter, J.T. George & J.H. Gauthier, 1987. "Measuring and modeling water imbibition into tuff" in Evans, D.D. & T.J. Nicholson [Eds.] *Flow and Transport Through Unsaturated Fractured Rock*, pp. 99-106. American Geophysical Union Monograph 42.

Philip, J. R. (1957). The theory of infiltration: 4. Sorptivity and algebraic infiltration equations. Soil science, 84(3), 257-264.

Tokunaga, T. K. (2020). Simplified Green-Ampt model, imbibition-based estimates of permeability, and implications for leak-off in hydraulic fracturing. Water Resources Research, 56(4), e2019WR026919.

Żołądek-Nowak, J., Milczarek, J., Fijał-Kirejczyk, I., Żołądek, J., & Jurkowski, Z. (2012). Transient Thermal Phenomena during Spontaneous Water Migration in Zeolite Beds. Acta Physica Polonica A, 122(2), 415-418.

SAND2023-14177C

This Low Yield Nuclear Monitoring (LYNM) research was funded by the National Nuclear Security Administration, Defense Nuclear Nonproliferation Research and Development (NNSA DNN R&D). The authors acknowledge important interdisciplinary collaboration with scientists and engineers from LANL, LLNL, NNSS, PNNL, and SNL.